Article

Numerical Simulations of Polymer Solution Droplet Impact on Surfaces of Different Wettabilities [†]

Moussa Tembely [1],[*] [ID], Damien Vadillo [2], Arthur Soucemarianadin [3] and Ali Dolatabadi [1],[*]

[1]   Department of Mechanical, Industrial, and Aerospace Engineering, Concordia University, Montreal, QC H3G 1M8, Canada

[2]   AkzoNobel, Research, Development and Innovation, Gateshead NE10 0EX, UK; damien.vadillo@akzonobel.com

[3]   Laboratory for Geophysical and Industrial Flow(LEGI), Grenoble University, Grenoble 38000, France; souce@ujf-grenoble.fr

[*]   Correspondence: moussa.tembely@concordia.ca (M.T.); ali.dolatabadi@concordia.ca (A.D.)

[†]   This paper is an extended version of a paper published at the 4th Micro and Nano Flows Conference, London, UK, 7–10 September 2014.

check for updates

Abstract: This paper presents a physically based numerical model to simulate droplet impact, spreading, and eventually rebound of a viscoelastic droplet. The simulations were based on the volume of fluid (VOF) method in conjunction with a dynamic contact model accounting for the hysteresis between droplet and substrate. The non-Newtonian nature of the fluid was handled using FENE-CR constitutive equations which model a polymeric fluid based on its rheological properties. A comparative simulation was carried out between a Newtonian solvent and a viscoelastic dilute polymer solution droplet. Droplet impact analysis was performed on hydrophilic and superhydrophobic substrates, both exhibiting contact angle hysteresis. The effect of substrates' wettability on droplet impact dynamics was determined the evolution of the spreading diameter. While the kinematic phase of droplet spreading seemed to be independent of both the substrate and fluid rheology, the recoiling phase seemed highly influenced by those operating parameters. Furthermore, our results implied a critical polymer concentration in solution, between 0.25 and 2.5% of polystyrene (PS), above which droplet rebound from a superhydrophobic substrate could be curbed. The present model could be of particular interest for optimized 2D/3D printing of complex fluids.

Keywords: droplet impact; viscoelasticity; volume of fluid method

1. Introduction

The dynamics of the impact and spreading of liquid drops onto a solid substrate is a highly active subject of research for both academic and industrial purposes. Indeed, these phenomena are widely encountered in everyday life, such as raindrops impacting on a surface. From an industrial perspective, there is much interest in the physics of non-Newtonian drop–surface interactions because of their wide range of applications. As such, a detailed knowledge of droplet impingement onto solid materials is required for the overall process development and improvement of many engineering operations. The impact of fluid drops on solid surfaces leads to different outcomes, such as partial or total spreading, recoil, or splashing [1]. One essential condition for the accurate placement of drops—a stringent requirement for technological applications—is the ability to control the maximum spreading diameter through different means. Although the problem has been considered from several angles for over 50 years, it is only during the past 10 years that repeatable and consistent results have been reported both on well-characterized homogenous substrates and on purpose-designed media

with either chemical or topological heterogeneities [2,3]. Very recently, Antonini et al. [4] performed a comprehensive study of the impact of drops on hydrophobic and superhydrophobic surfaces so as to help select the appropriate substrate for a given application. Complex fluid droplet impact has gained attention recently due to the key role it plays in applications ranging from 3D printing, polymer light-emitting diode technology, and lab-on-chip technology, to biotechnology for protein engineering [5–10]. The liquids involved in these processes are likely to exhibit non-Newtonian properties, such as viscoelasticity, which results from adding flexible polymers to solvent liquids. In order to address these challenges, numerical tools are essential for the accurate modeling of droplet dynamics on surfaces exhibiting different wettabilities.

Numerical models to handle droplet impact have been investigated since the initial work by Fukai et al. [11] based on the volume of fluid (VOF) method first introduced by Hirt and Nichols [12]. Since then, a wide range of numerical techniques have been developed for computing multiphase flow with moving interfaces, including, for example, the level set method [13], the front tracking method [14], and the lattice–Boltzmann method [15,16]. Among those cited, the VOF method has enjoyed a rather special place in the simulation of drop spreading for many reasons. These include its inherent mass conservation property, its suitability for problems where large surface topology changes occur, the ease of its implementation, and its reduced computational costs. However, it may be less accurate in interface calculations than, for example, the level set method, which is particularly adapted for resolving intricate topological changes of interfaces. In spite of this limitation, it is still the most preferred method for computations of drop impact and spreading where quite strong interfacial effects occur both at the substrate level and at the free surface of the drop [17,18]. To be more complete on the issue of numerical simulations of drop impact, it should be mentioned that the lattice–Boltzmann and phase field methods have recently been used for characterizing drop impact behavior. Additionally, another approach using the coupled level set and volume of fluid (CLSVOF) formulation has been implemented, with the VOF method dealing with the interface motion and the level set technique handling surface tension effects. This approach also remedied the problem of mass conservation typically encountered with level set methods.

A fundamental understanding of the droplet dynamics of complex fluids is a key element for future breakthroughs in the growing domain of micro-fabrication and micro-fluidics [7,9]. Regarding droplet impact, the question of whether a droplet will be deposited on the substrate or will eventually rebound is of particular interest, and a full understanding of the entire droplet impact dynamic is required.

Although Newtonian droplet impact has been extensively studied in the literature, the non-Newtonian viscoelastic droplet impact—despite its plethora of useful applications—has been only loosely documented both experimentally and numerically, even though recent works, showing an increasing interest for these fluids, make them an active research area. A finite element method was pioneered in Reference [19] to model the die swell of an Oldroyd-B fluid through an ad-hoc iterative technique for the free surface, based on the kinematic condition. The split Lagrangian–Eulerian method was extended by [20] to study viscoelastic jet breakup. Recently, Reference [21] simulated free surface flow using both marker-and-cell (MAC) and finite difference (FD) techniques. In addition, a mesh-free method using the smoothed particle hydrodynamics (SPH) technique has been applied to model an Oldroyd-B drop impact in 2D while neglecting the surface tension [22]. These different techniques neglect both the surface tension and the dynamic contact angle during spreading, along with the presence of air. Additionally, it is worth noting the interface-capturing techniques used to model non-Newtonian free surface flow such as the level set method [23] or the phase field method [24]. Finally, a one-dimensional approach [25] to model free surface flow of non-Newtonian fluid using an arbitrary Lagrangian–Eulerian (ALE) method should be mentioned, as it has shown good results in modeling filament thinning using the FENE-CR model.

Although the low viscosity of dilute polymers are of particular interest in inkjet fluids [26,27], it is only recently that they have been experimentally investigated using a controlled stretching

rheometer [28]. The present work benefitted from the rheological characterization of these fluids to optimize the simulation.

Most numerical studies have considered polymeric internal flow, but few have considered droplet interaction with a solid substrate. Within the VOF framework, the present model (accounting for the substrate hysteresis) investigated viscoelastic droplets impact using a single mode FENE-CR model in an axisymmetric configuration. The numerical model enabled the effect of monodisperse polymer concentration in solution and the resulting liquid droplet dynamics on both hydrophilic and superhydrophobic surfaces to be investigated.

The paper is organized as follows. Section 2 details the equations governing the numerical model and the polymers solutions' rheological properties. After validation of the model in the Newtonian case, the main results regarding the polymer droplet impact on hydrophilic and superhydrophobic flat surfaces are discussed in Section 3. Section 4 concludes the paper.

2. Methodology

2.1. Numerial Methods

The equations governing the impact of a non-Newtonian droplet are based on the discretization of the mass and momentum equations within the VOF framework. In the present work, the focus was be on modeling the impact and spreading of a droplet of dilute polymer solution which displays a viscoelastic behavior. Therefore, the momentum conservation equation incorporated this effect through an additional stress tensor (τ_p), and the governing equations can be written as follows:

$$\nabla.\boldsymbol{V} = 0 \tag{1}$$

$$\frac{\partial(\rho\boldsymbol{V})}{\partial t} + \nabla.(\rho\boldsymbol{V}\boldsymbol{V}) = -\nabla p + \rho\boldsymbol{g} + \nabla.(\eta_s\nabla\boldsymbol{V}) + \nabla.\boldsymbol{\tau}_p + \gamma\kappa\nabla\alpha \tag{2}$$

where κ is the curvature of the free surface, γ is the surface tension, α is the phase fraction of the liquid phase, η_s is the viscosity of the solvent, g is the gravity acceleration, p is the pressure, and V the velocity.

In Equation (2), the continuum surface force (CSF) method of Brackbill et al. [29] was used to model the surface tension as a body force acting only on interfacial numerical cells, and the mean curvature at the interface is given by

$$\kappa = -\nabla.\left(\frac{\nabla\alpha}{|\nabla\alpha|}\right) \tag{3}$$

The outcome of an impacting drop is affected by various factors including droplet properties and kinematic and surface characteristics. In the present paper, the impact of a droplet of diameter D_0 impacting at an initial velocity of V_0 was simulated. To analyze droplet impact dynamics, we used the spreading factor, defined as the ratio between the spreading diameter and droplet initial diameter (D_0). In addition, the time was made dimensionless using the kinematic time scale $t_\mathrm{c} = D_0/V_0$.

In order to model the polymer solution rheology, we used the dumbbell approximation based on a finitely extensible nonlinear elastic fluid in Reference [30], known as FENE-CR. This choice of FENE-CR was motivated by its superior performance for modeling viscoelastic behavior, as we have previously shown in the context of filament thinning and stretching [25,31,32]. The equation relating the stress tensor to conformation tensor A was expressed as follows:

$$\kappa = -\nabla.\boldsymbol{\tau}_p = Gf(\,R\,)\,(\boldsymbol{A} - I) \tag{4}$$

where the elastic modulus is denoted by G and $f(R)$ the finite extensibility factor is given by

$$f(R) = \frac{1}{1 - R/L^2} \tag{5}$$

which relates the finite extensibility parameter L, which corresponds to the maximum possible extension of the dumbbell, to the parameter $R = \text{Tr}(A)$.

The polymer impact on the flow behaviour can be expressed through the constitutive equations based the evolution of the conformation tensor:

$$\frac{dA}{dt} - \nabla V^T.A - A.\nabla v = -\frac{f(R)}{\lambda}(A - I) \tag{6}$$

where λ denotes the relaxation time and I the identity tensor.

Finally, the transport of the phase fraction equation was simulated through an interface compression method:

$$\frac{\partial \alpha}{\partial t} + V\nabla\alpha + \nabla.[V_c\alpha(1 - \alpha)] = 0 \tag{7}$$

The interface compression speed V_c, describing the relative velocity at the free surface between the fluids, followed the equation below [33]:

$$V_c = n_f \, min\left[C_\alpha \frac{\phi_f}{S_f}, max\left(\frac{\phi_f}{S_f}\right)\right] \tag{8}$$

where S_f and ϕ_f represent cell surface area and mass flux, respectively, while the coefficient C_α, set here to 1, defines the degree of compression at the interface. It is worth noting that the adoption of an interface compression scheme avoids the tedious geometrical reconstruction of the interface habitually done in implementation of the VOF method. In addition, the algebraic method used here can readily be extended to unstructured meshes. Further details of the numerical discretization schemes and techniques can be found in Reference [34].

Within the VOF framework, the different physical parameters in each cell of the domain were expressed through the liquid fraction as follows:

$$\xi = \alpha\xi_{liquid} + (1 - \alpha)\xi_{gas} \tag{9}$$

where ξ represents any physical properties, such as the density, velocity, or viscosity, for both the liquid and gas phases.

To handle the liquid–substrate interaction, a more physically-based dynamic contact angle model was used. Droplet impact dynamics are highly controlled by the manner in which its dynamic contact angle is modeled. In the present work, Kistler's dynamic contact angle model [34,35] was implemented:

$$\theta_d = f_H[Ca + f_H^{-1}(\theta_E)] \tag{10}$$

with the Hoffman function expressed as

$$f_H(s) = arccos\left\{1 - 2\tanh\left[5.16\left[\frac{s}{1 + 1.31s^{0.99}}\right]^{0.706}\right]\right\} \tag{11}$$

where the capillary number $Ca = \mu U_{cl}/\gamma$, in which U_{cl} corresponds to the contact line velocity, was numerically approximated by taking the velocity within the first cell above the substrate. The effect of the surface hysteresis was accounted for by replacing the equilibrium contact angle θ_E in Equation (9) by either the receding contact angle θ_R or the advancing contact angle θ_A according to the direction of the triple line velocity. By adopting this approach, our model became sensitive to the substrate hysteresis, which plays a significant role in simulating droplet impacts on surfaces with varied wettabilities. It is worth noting that unlike in Reference [36], the presented model did not rely heavily on experimental measurements of the dynamic contact angle evolution in order to match a given experiment.

Finally, the governing Equations (1)–(11) were implemented in OpenFOAM/C++ using second order linear upwind-biased schemes. The simulations (in axisymmetric geometry) were performed in

parallel using the domain decomposition method. The pressure implicit with splitting of operators (PISO) algorithm was used to calculate the pressure, while the evolution of the conformation tensor was solved using a preconditioned bi-conjugate gradient technique; further details on implementation and discretization can be found in our previous work in References [10,34,37]. The convergence criteria set for the pressure, velocity, and conformation tensor fields were of the order of 10^{-6}.

2.2. Polymer Solution and Substrates Properties

In order to evaluate our numerical model, a viscoelastic liquid and its properties were measured based on a "Cambridge Trimaster" filament stretching and thinning experimental set-up [28]. This extensional rheometer proceeded by performing filament stretching at a constant velocity for a liquid initially placed between two pistons of initial diameter 1.2 mm. The two pistons, which operate on opposite sides of a belt, move away from each other at a prescribed distance, letting the mid-filament remain in a central position. The ensuing measurements of the filament mid-diameter allows accurate estimation the relaxation time of the liquid, which has been shown previously to be crucial in numerical modeling of filament thinning dynamics [25].

The numerical simulation investigated a Newtonian solvent—diethyl phthalate (DEP)—in addition to a polymer solution consisting of polystyrene (PS), 110,000 g/mol, dissolved into the DEP solvent. Table 1 presents the interfacial surface tension and viscosity values of the two liquids.

Table 1. Liquid physical properties. DEP: diethyl phthalate, PS: polystyrene.

Liquids	Interfacial Surface Tension (mN/m)	Viscosity (mPa.s)
DEP	37	14
DEP + 2.5% PS	37	31

Finally, the relaxation time measured from the polymer solution, DEP + 2.5 wt % PS, was λ = 1.19 ms, while the extensibility parameter *L*, accounting for the liquid physical properties, was taken as *L* = 15 [25].

Regarding fluid–substrate interaction, we considered two types of substrate in the numerical experiment, hydrophilic and superhydrophobic, the properties of which were similar to the aluminum and WX2100 properties for a water droplet, respectively [38]. Experimentally, it may be challenging to find a substrate exhibiting those chemical properties with respect the DEP and DEP + 2.5 wt. % PS, though the aim of this study was to highlight the relevant features in viscoelastic droplet dynamics, which have been poorly numerically documented in the literature, especially with the added effect of substrate hysteresis. The contact angles (CAs) consisting of the equilibrium contact angles, in addition to the hysteresis with the advancing and receding contact angles of these two substrates, are given in Table 2.

**Table 2.** Substrate contact angles (CAs).

| Substrate	Equilibrium CA (°)	Advancing CA (°)
Hydrophilic (H)	74	90
Superhydrophobic (SH)	154	162

3. Results

3.1. Validation of Newtonian Droplet Impact Dynamics

We first tested the model in a Newtonian case for validation. For this purpose, we have provided a comparison of the VOF method using our modified Kistler's model to tackle the challenging case of droplet impact on a surface with contact angle hysteresis (CAH). The comparison was performed

with an experiment performed in Antonini et al. [39] for the impact of a 2.5 mm diameter droplet impacting at 1 m/s with receding and advancing contact angles of 108°/169°. The results are shown in Figures 1 and 2 for the transient profile and spreading diameter evolution, respectively. We observed a good agreement between the experiment and simulation of the droplet upon impact on a surface exhibiting a significant contact angle hysteresis, CAH = 61°, highlighting the robustness and capability of our model and paving the way for an accurate assessment of the impact of non-Newtonian fluids.
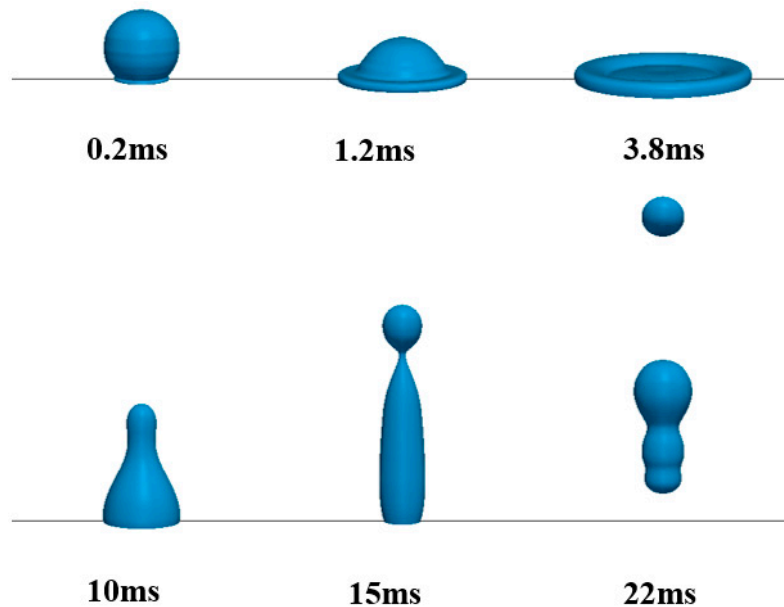
Figure 1. Transient profiles of a Newtonian droplet impacting a superhydrophobic surface.
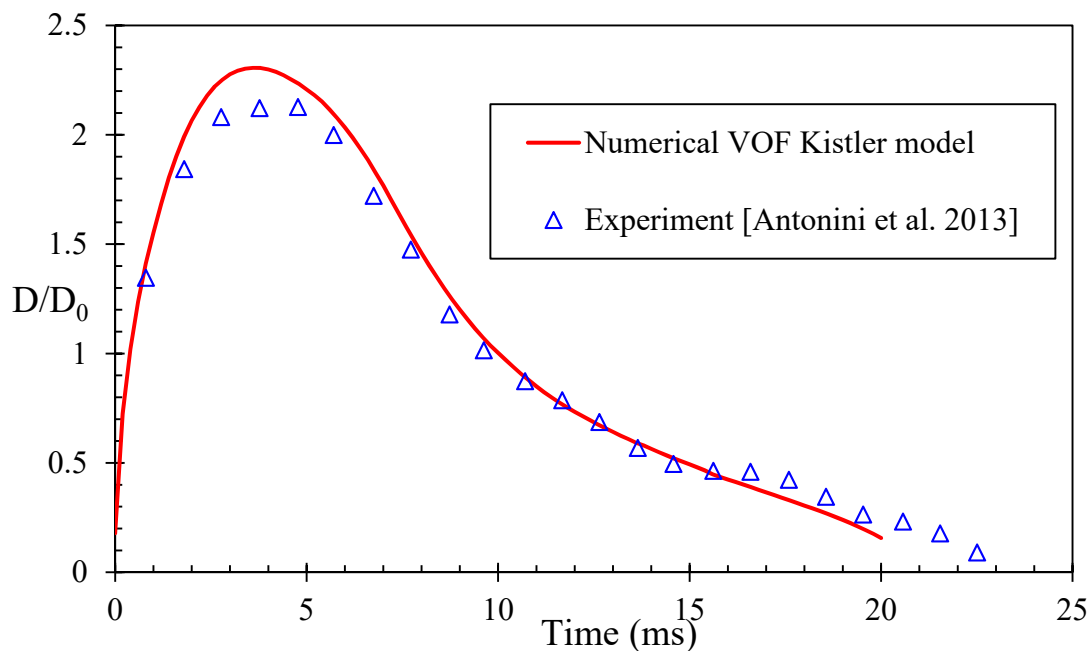

Figure 2. Comparison between simulation and experiment of the dimensionless spreading diameter evolution of a droplet upon impact on a superhydrophobic substrate with hysteresis. VOF: volume of fluid.
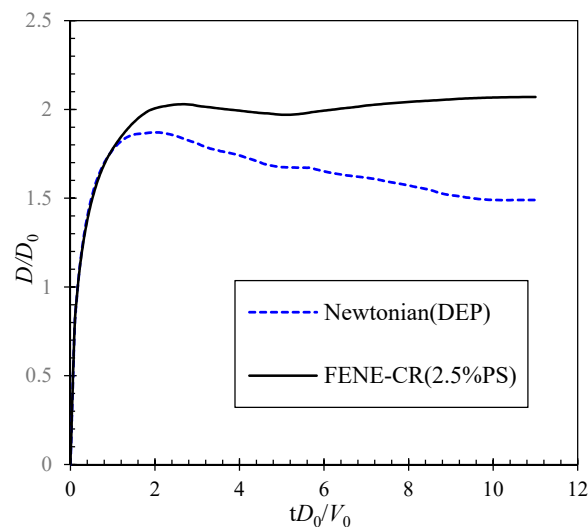
3.2. Impact of Polymer Solution Droplet

3.2.1. Hydrophilic Surface

We performed a comparative simulation of a Newtonian and a polymer solution droplet impact on a hydrophilic surface (Table 2). The transient evolution of 1 mm diameter drop at a velocity of 1 m/s is shown in Figure 3. The left-hand side corresponds to the Newtonian liquid, while the polymer droplet is shown on the right hand-side. We plotted the dimensionless spreading diameter (D/D_0) function of the dimensionless time ($t_c = t \, V_0/D_0$). We observed that during the kinematic phase ($t_c < 1$), droplet spreading seemed to be independent of the fluid model (Figure 4). However, at subsequent phases of the two droplets' spreading, we observed a much more marked difference between the two cases. Additionally, the viscoelastic liquid droplet displayed little oscillation while having a greater maximum spreading diameter, due to the dominance of the elastic normal stress over of the surface tension, which favored retraction. Interestingly, the liquid flowing out of the droplet center towards its periphery seemed to behave similarly to the filament thinning and stretching situation we reported in Reference [25].
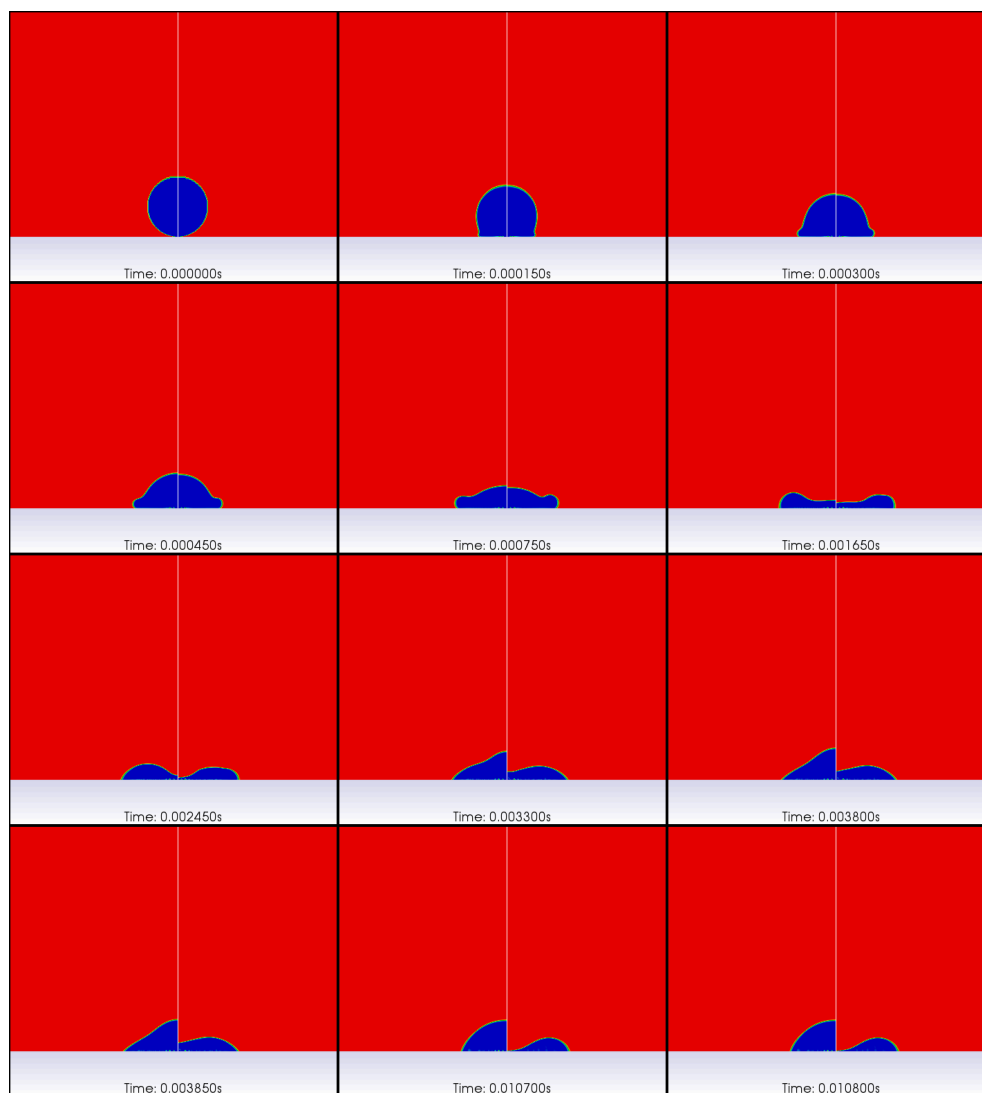
Figure 3. A comparative simulation of a 1 mm diameter droplet impacting at 1 m/s on a hydrophilic substrate between (**right**) a Newtonian solvent DEP and (**left**) polymer solution, DEP + 2.5 wt. % PS.

Figure 4. Evolution of the dimensionless spreading diameter on the hydrophilic surface.
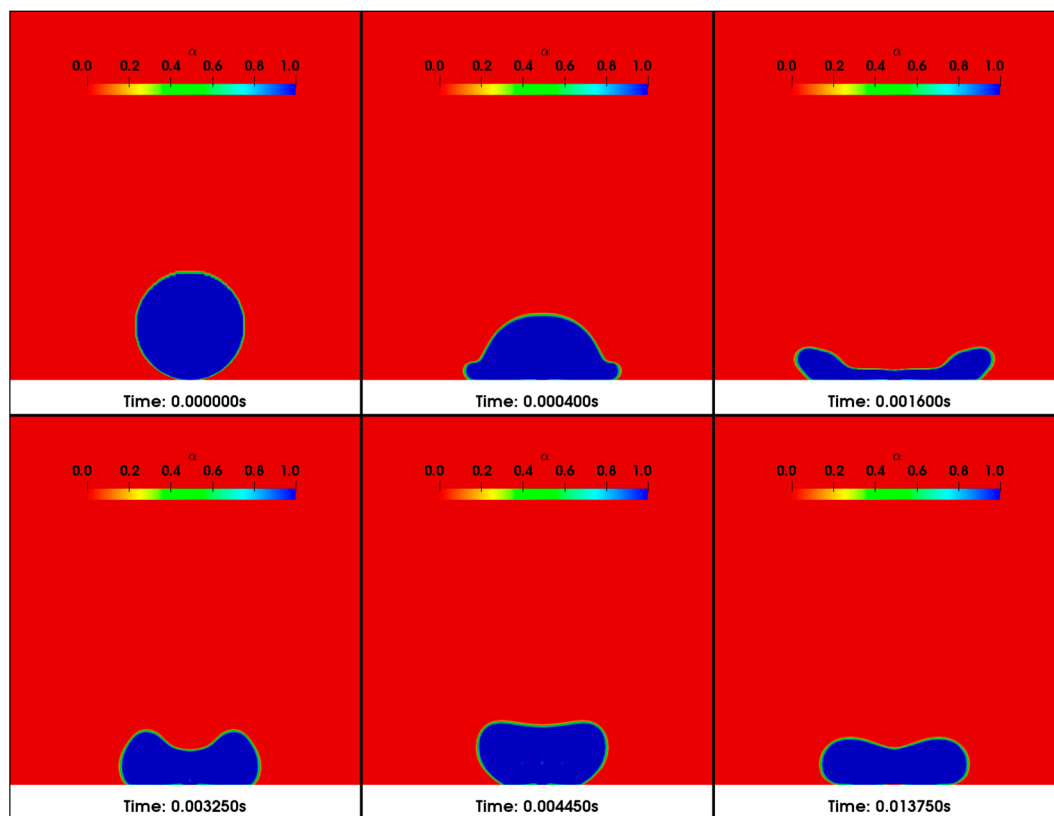
3.2.2. Superhydrophobic Surface

We simulated the impact of a 1 mm droplet at 1 m/s on a superhydrophobic (SH) substrate comparing a Newtonian and polymer solution, which was modeled by a FENE-CR fluid. Comparative transient profiles between the two cases are depicted in Figure 5. The left-hand side corresponds to the Newtonian DEP solvent, while the right-hand side represents the polymer solution, which consisted of a dilution of polymer (PS) into the solvent. The addition of a minute quantity of polymer to a Newtonian liquid has been found to affect droplet dynamics, mainly during the recoiling stage for the impact conditions that were investigated in the present work. The kinetic energy of a impacting droplet is converted to the elastic and surface energy; that stored energy contributes to droplet retraction and rebound on superhydrophobic surface, after partial dissipation by viscous effect. As expected, the Newtonian (DEP) droplet rebounded and detached after impact on the superhydrophobic substrate; however, the rebound was suppressed with the dilute polymer solution (DEP + 2.5 wt. % PS), where the high elongational viscosity dissipated much of the drop kinetic energy during the spreading phase. As the Newtonian DEP droplet rebounded from the superhydrophobic surface, the dilute polymer settled at its equilibrium position during the wetting phase, as depicted in Figure 6.

Finally, the contrast between the Newtonian and the polymer solution behavior is quantified in Figure 7 by the dimensionless spreading diameter evolution. For superhydrophobic substrate, it is worth noting that the maximum spreading diameter in contact with substrate should not be confused with the maximum (deformation) diameter. The latter was higher for the viscoelastic fluid than the Newtonian one. In addition, we found that with a much lower concentration of polymer (DEP + 0.25 wt. % PS), the droplet bounced back again on the superhydrophobic substrate, which exhibited per se a higher retraction energy (Figure 7). Therefore, this implies the existence of a critical polymer concentration between 0.25 wt. % PS and 2.5 wt. % PS, above which droplet rebound can be suppressed on a superhydrophobic surface. The capability of our numerical model to retrieve such a feature is of particular interest for various processes, such as nutrients deposited as spray on plants and 2D/3D drop-on-demand printing.
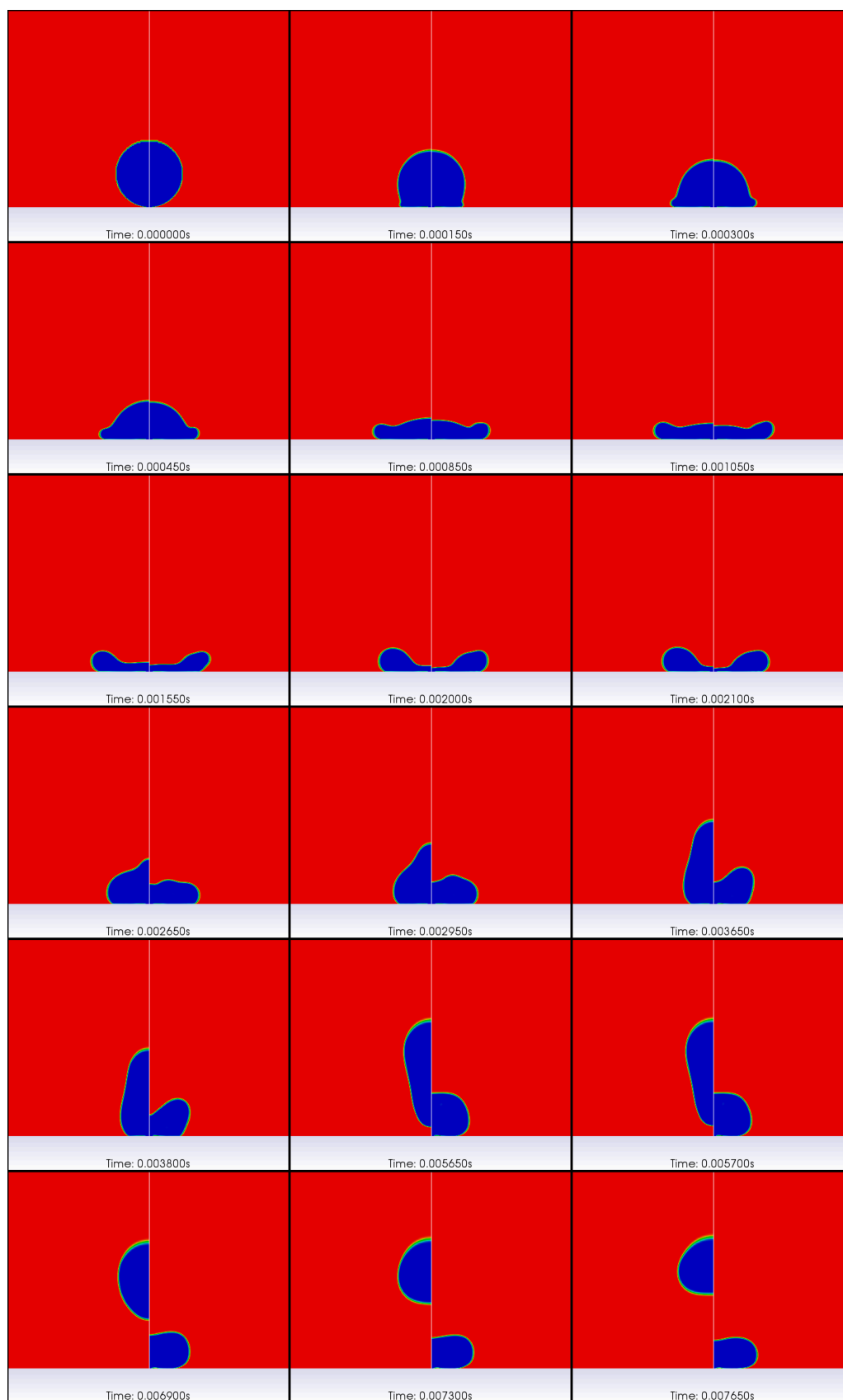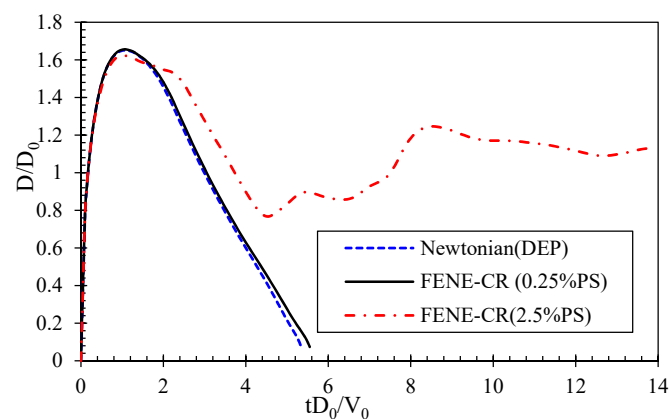
Figure 5. Simulated comparison between (**right**) the Newtonian solvent DEP and (**left**) viscoelastic polymer solution, DEP + 2.5 wt. % PS, for the impact of a 1 mm diameter droplet at 1 m/s on the superhydrophobic substrate.

Figure 6. Impact of a 1 mm droplet of polymer solution, DEP + 2.5 wt. % PS, at 1 m/s on the superhydrophobic substrate.

Figure 7. Simulated spreading diameter of 1 mm droplets of a Newtonian (DEP) fluid and two polymer solutions, DEP + 0.25 wt. % and DEP + 2.5 wt. % PS, impacting at 1 m/s.

4. Conclusions

Numerical simulations of droplet impact on different substrates based the VOF method were performed for both Newtonian and polymer solutions. The liquid–substrate interaction was also accounted for with a more realistic dynamic contact angle, as opposed to solely relying on the equilibrium contact angle. The constitutive equations considered for the viscoelastic fluids came from the FENE-CR model. While no noticeable difference was found in the early stages of droplet impact (beyond the kinematic phase), we observed that the substrate and fluid viscoelasticity influence became much more dominant on droplet dynamics during the recoiling phase particularly. The results of the simulation indicated that the dilute polymer solution droplet had a higher spreading diameter

compared to a Newtonian solvent on a hydrophilic substrate. This can be explained by the dominance of the elastic normal stress over both the kinetic energy dissipation and surface tension force, which tends to favor droplet retraction. In addition, the existence of a critical polymer concentration—at which a droplet may no longer detach, even on superhydrophobic substrates—was inferred. The present model, based on a single mode FENE-CR fluid, could be extended to multimode constitutive models, along with tailored experiments for a comprehensive description of polymer droplet impact.

Author Contributions: M.T., D.V., A.S. and A.D. designed the study. M.T. performed the study and wrote the paper. All the authors contributed to the paper.

Conflicts of Interest: The authors declare no conflict of interest.

References

1. Rioboo, R.; Marengo, M.; Tropea, C. Time evolution of liquid drop impact onto solid, dry surfaces. *Exp. Fluids* **2002**, *33*, 112–124. [CrossRef]
2. Mock, U.; Michel, T.; Tropea, C.; Roisman, I.; Rühe, J. Drop impact on chemically structured arrays. *J. Phys. Condens. Matter* **2005**, *17*, S595–S605. [CrossRef]
3. Vadillo, D.C.; Soucemarianadin, A.; Delattre, C.; Roux, D.C.D. Dynamic contact angle effects onto the maximum drop impact spreading on solid surfaces. *Phys. Fluids* **2009**, *21*, 122002. [CrossRef]
4. Antonini, C.; Amirfazli, A.; Marengo, M. Drop impact and wettability: From hydrophilic to superhydrophobic surfaces. *Phys. Fluids* **2012**, *24*, 102104. [CrossRef]
5. Tembely, M.; Vadillo, D.; Mackley, M.R.; Soucemarianadin, A. Towards an optimization of DOD printing of complex fluids. *Int. Conf. Digit. Print. Technol.* **2011**, *2011*, 86–92.
6. Clemens, W.; Fix, W.; Ficker, J.; Knobloch, A.; Ullmann, A. From polymer transistors toward printed electronics. *J. Mater. Res.* **2004**, *19*, 1963–1973. [CrossRef]
7. Xu, J.; Attinger, D. Drop on demand in a microfluidic chip. *J. Micromech. Microeng.* **2008**, *18*, 065020. [CrossRef]
8. Ottnad, T.; Kagerer, M.; Irlinger, F.; Lueth, T.C. Modification and further development of a drop on demand printhead for wax enabling future 3D-printing and rapid prototyping. In Proceedings of the 2012 IEEE/ASME International Conference on Advanced Intelligent Mechatronics (AIM), Kaohsiung, Taiwan, 11–14 July 2012; pp. 117–122.
9. Joensson, H.N.; Andersson-Svahn, H. Droplet microfluidics—A tool for protein engineering and analysis. *Lab Chip* **2011**, *11*, 4144. [CrossRef]
10. Tembely, M.; AlSumaiti, A.M.; Jouini, M.S.; Rahimov, K. The effect of heat transfer and polymer concentration on non-Newtonian fluid from pore-scale simulation of rock X-ray micro-CT. *Polymers* **2017**, *9*, 509. [CrossRef]
11. Fukai, J.; Zhao, Z.; Poulikakos, D.; Megaridis, C.M.; Miyatake, O. Modeling of the deformation of a liquid droplet impinging upon a flat surface. *Phys. Fluids A Fluid Dyn.* **1993**, *5*, 2588–2599. [CrossRef]
12. Hirt, C.; Nichols, B. Volume of fluid (VOF) method for the dynamics of free boundaries. *J. Comput. Phys.* **1981**, *39*, 201–225. [CrossRef]
13. Sussman, M.; Smereka, P.; Osher, S. A Level Set Approach for Computing Solutions to Incompressible Two-Phase Flow. *J. Comput. Phys.* **1994**, *114*, 146–159. [CrossRef]
14. Tryggvason, G.; Bunner, B.; Esmaeeli, A.; Juric, D.; Al-Rawahi, N.; Tauber, W.; Han, J.; Nas, S.; Jan, Y.J. A Front-Tracking Method for the Computations of Multiphase Flow. *J. Comput. Phys.* **2001**, *169*, 708–759. [CrossRef]
15. Shan, X.; Doolen, G. Multicomponent lattice-Boltzmann model with interparticle interaction. *J. Stat. Phys.* **1995**, *81*, 379–393. [CrossRef]
16. Dalgamoni H., N. and Yong X. Axisymmetric lattice Boltzmann simulation of droplet impact on solid surfaces. *Phys. Rev. E.* **2018**, *98*, 013102. [CrossRef] [PubMed]
17. Roisman, I.V.; Opfer, L.; Tropea, C.; Raessi, M.; Mostaghimi, J.; Chandra, S. Drop impact onto a dry surface: Role of the dynamic contact angle. *Colloids Surf. A Physicochem. Eng. Asp.* **2008**, *322*, 183–191. [CrossRef]

18. Šikalo, Š.; Wilhelm, H.-D.; Roisman, I.V.; Jakirlić, S.; Tropea, C. Dynamic contact angle of spreading droplets: Experiments and simulations. *Phys. Fluids* **2005**, *17*, 062103. [CrossRef]

19. Crochet, M.J.; Keunings, R. Finite element analysis of die swell of a highly elastic fluid. *J. Nonnewton. Fluid Mech.* **1982**, *10*, 339–356. [CrossRef]

20. Morrison, N.F.; Harlen, O.G. Viscoelasticity in inkjet printing. *Rheol. Acta* **2010**, *49*, 619–632. [CrossRef]

21. Tomé, M.F.; Paulo, G.S.; Pinho, F.T.; Alves, M.A. Numerical solution of the PTT constitutive equation for unsteady three-dimensional free surface flows. *J. Nonnewton. Fluid Mech.* **2010**, *165*, 247–262. [CrossRef]

22. Fang, J.; Owens, R.G.; Tacher, L.; Parriaux, A. A numerical study of the SPH method for simulating transient viscoelastic free surface flows. *J. Nonnewton. Fluid Mech.* **2006**, *139*, 68–84. [CrossRef]

23. Yu, J.-D.; Sakai, S.; Sethian, J.A. Two-phase viscoelastic jetting. *J. Comput. Phys.* **2007**, *220*, 568–585. [CrossRef]

24. Yue, P.; Feng, J.J. Phase-field simulations of dynamic wetting of viscoelastic fluids. *J. Nonnewton. Fluid Mech.* **2012**, *189*, 8–13. [CrossRef]

25. Tembely, M.; Vadillo, D.; MacKley, M.R.; Soucemarianadin, A. The matching of a "one-dimensional" numerical simulation and experiment results for low viscosity Newtonian and non-Newtonian fluids during fast filament stretching and subsequent break-up. *J. Rheol.* **2012**, *56*, 159–183. [CrossRef]

26. Dong, H.; Carr, W.W.; Morris, J.F. An experimental study of drop-on-demand drop formation. *Phys. Fluids* **2006**, *18*, 072102. [CrossRef]

27. Hoath, S.D.; Vadillo, D.C.; Harlen, O.G.; McIlroy, C.; Morrison, N.F.; Hsiao, W.-K.; Tuladhar, T.R.; Jung, S.; Martin, G.D.; Hutchings, I.M. Inkjet printing of weakly elastic polymer solutions. *J. Nonnewton. Fluid Mech.* **2014**, *205*, 1–10. [CrossRef]

28. Vadillo, D.C.; Tuladhar, T.R.; Mulji, A.C.; Jung, S.; Hoath, S.D.; Mackley, M.R. Evaluation of the inkjet fluid's performance using the "Cambridge Trimaster" filament stretch and break-up device. *J. Rheol.* **2010**, *54*, 261–282. [CrossRef]

29. Brackbill, J.; Kothe, D.; Zemach, C. A continuum method for modeling surface tension. *J. Comput. Phys.* **1992**, *100*, 335–354. [CrossRef]

30. Chilcott, M.D.; Rallison, J.M. Creeping flow of dilute polymer solutions past cylinders and spheres. *J. Nonnewton. Fluid Mech.* **1988**, *29*, 381–432. [CrossRef]

31. Vadillo, D.C.; Tembely, M.; Morrison, N.F.; Harlen, O.G.; MacKley, M.R.; Soucemarianadin, A. The matching of polymer solution fast filament stretching, relaxation, and break up experimental results with 1D and 2D numerical viscoelastic simulation. *J. Rheol.* **2012**, *56*, 1491–1516. [CrossRef]

32. Mackley, M.R.; Butler, S.A.; Huxley, S.; Reis, N.M.; Barbosa, A.I.; Tembely, M. The observation and evaluation of extensional filament deformation and breakup profiles for Non Newtonian fluids using a high strain rate double piston apparatus. *J. Nonnewton. Fluid Mech.* **2017**, *239*, 13–27. [CrossRef]

33. Rusche, H. Computational Fluid Dynamics of Dispersed Two-Phase Flows at High Phase Fractions. Ph.D. Thesis, Imperial College of Science, Technology and Medicine, London, UK, 2002.

34. Tembely, M.; Attarzadeh, R.; Dolatabadi, A. On the numerical modeling of supercooled micro-droplet impact and freezing on superhydrophobic surfaces. *Int. J. Heat Mass Transf.* **2018**, *127*, 193–202. [CrossRef]

35. Kistler, S.F. Hydrodynamics of Wetting. In *Wettability*; Berg, J.C., Ed.; CRC Press: Boca Raton, FL USA, 1993.

36. Yokoi, K.; Vadillo, D.; Hinch, J.; Hutchings, I. Numerical studies of the influence of the dynamic contact angle on a droplet impacting on a dry surface. *Phys. Fluids* **2009**, *21*, 072102. [CrossRef]

37. Jadidi, M.; Tembely, M.; Moghtadernejad, S.; Dolatabadi, A. A coupled level set and volume of fluid method in openfoam with application to compressible two-phase flow. In Proceedings of the 22nd Annual Conference of the CFD Society of Canada, Toronto, ON, Canada, 1–4 June 2014.

38. Graham, P.J.; Farhangi, M.M.; Dolatabadi, A. Dynamics of droplet coalescence in response to increasing hydrophobicity. *Phys. Fluids* **2012**, *24*, 112105. [CrossRef]

39. Antonini, C.; Villa, F.; Bernagozzi, I.; Amirfazli, A.; Marengo, M. Drop Rebound after Impact: The Role of the Receding Contact Angle. *Langmuir* **2013**, *29*, 16045–16050. [CrossRef]